Electronic Supplementary Information

to the paper

Prebiotic Synthesis at Impact Craters: the Role of Fe-Clays and Iron Meteorites

by

Adam Pastorek,[a,b] Jana Hrnčířová,[a,c] Luboš Jankovič,[d] Lukáš Nejdl,[e] Svatopluk Civiš,[a] Ondřej Ivanek,[a] Violetta Shestivska,[a] Antonín Knížek,[a,c] Petr Kubelík,[a,f] Jiří Šponer,[g] Lukáš Petera,[a,c] Anna Křivková,[a,b] Giuseppe Cassone,[g] Markéta Vaculovičová,[e,†] Judit E. Šponer,[g,†] and Martin Ferus[a,†]

[a.] *J. Heyrovský Institute of Physical Chemistry, Czech Academy of Sciences, Dolejškova 3, 182 23 Prague 8, Czech Republic*
[b.] *Faculty of Nuclear Sciences and Physical Engineering, Czech Technical University in Prague, Břehová 78/7, 115 19 Prague 1, Czech Republic*
[c.] *Charles University in Prague, Faculty of Science, Chemical institute, Hlavova 2030/8, 128 00 Prague 2, Czech Republic*
[d.] *Institute of Inorganic Chemistry, Slovak Academy of Sciences, Dúbravskácesta 9, 845 36 Bratislava 45, Slovak Republic*
[e.] *ÚCB AF, Mendel University in Brno, Zemědělská 1, 613 00 Brno, Czech Republic*
[f.] *Institute of Physics, Czech Academy of Sciences, Na Slovance 1999/2, 182 21 Prague 8, Czech Republic*
[g.] *Institute of Biophysics of the Czech Academy of Sciences, Královopolská 135, 612 65 Brno, Czech Republic*
† Corresponding authors. E-mails: martin.ferus@jh-inst.cas.cz (MF), marketa.vaculovicova@mendelu.cz (MV), judit@ncbr.muni.cz (JES)

Content:

SI.Catalysts

Table S1 summarizes the composition of catalyst mixtures used in the current study. As Ni/Fe meteorite we have used a specimen of Campo del Cielo meteorite with the following chemical composition: 92.9% Fe, 6.7% Ni, 0.4% Co and trace amounts 90 ppm of Ga, 392 ppm of Ge and 3.2 ppm of Ir (purchased from Špalek Minerals, Doksy u Kladna, Czech Republic). Ferric oxide Fe_2O_3 (Sigma Aldrich, powder, < 5 μm, ≥96%, CAS 1309-37-1). For description and characterization of the clays used seethe next section. The experiments were performed using ≈0.1 g of solid catalyst and 2 mL of formamide (Sigma Aldrich, molecular biology grade > 99.5 %, CAS 75-12-7).

Table S1. Composition of the catalyst mixtures used for thermolysis of formamide

Number of experiment in Table 1 (main text)	*Catalyst composition*
5	0.1g Fe-clay +0.01 g Ni/Fe-meteorite
6	0.1 g Na-clay + 0.01 g Ni/Fe-meteorite
7	0.1 g H-clay + 0.01 g Ni/Fe meteorite
10	0.1g Fe_2O_3 + 0.01 g Ni/Fe-meteorite

Clays – material properties and characterization

Natural sodium montmorillonite (abbreviated as Na-clay) was acquired from Kunimine Industries (Japan) and ferruginous smectite (Fe-clay) was obtained from the Source Clay Repository of the Clay Mineral Society (Grand County, Washington, USA). The fine fractions (less than 2 μm) were separated by sedimentation and centrifugation after disaggregation in deionized water (18 $M\Omega \cdot cm^{-1}$ resistivity). The samples have been purified via multiplied sediment fractionation to less than 2 μm particle size. The purified sodium clay was suspended in deionized water for 24 h under stirring using a magnetic stir-bar and plate to hydrate the clay. The suspension was prepared by mixing 10 g of clay with 500 mL of deionized water in a 2 L beaker. After suspending the clay, 500 mL 2M hydrochloric acid (HCl) was added under

vigorous stirring and after 1 hour of additional stirring at 20^{o}C the reaction mixture was centrifuged for 10 minutes at 4000 RPM. The supernatant liquid was discarded and the pellet was resuspended with 1 L of deionized water, and the product (H-clay) was retrieved by repetitive centrifugation and washing with deionized water to remove the excess of acid (HCl) and soluble salt (NaCl) formed in the course of the cation-exchange procedure.

$$\text{Na–clay} + \text{HCl} \rightarrow \text{H–clay} + \text{NaCl}$$

Table S2 shows the elemental composition of the clays used in this study. The data illustrate that in the purified Na-clay the charge of this dioctahedral mineral is dominantly located in the octahedral sheet due to significant substitution of aluminium with magnesium. Table S2 also shows that there is a very little change in the proportion of Mg, Al, Si and Fe after treatment of the Na-clay with HCl indicating that the ion-exchange process did not damage the aluminosilicate framework of the clay. Results of the chemical analysis also illustrate that in the ferruginous smectite (Fe-clay) the structural iron substitutes for majority of the structural Al^{3+}centers located in the octahedral sheet.

Table S2: Elemental analyses of the clays used in this study

Target analysis (%)	**Na-Clay**	**H-clay**	**Fe-clay**
SiO_2	61.67	63.98	51.63
Al_2O_3	22.18	22.12	9.18
Fe_2O_3	1.96	1.92	26.47
MgO	2.78	2.64	1.46
CaO	0.15	0.02	2.76
Na_2O	3.52	0.08	0.09
Ignitionloss	7.67	8.96	8.34

The ignition loss in Table S2 stands for mass loss in percent due to heating in flame (annealing). In order to test purity of the clays, all the samples have also been characterized by solid phase FTIR spectroscopy and XRD analysis. The IR spectra of fine fractions, depicted in Figure S1, Panel A are very similar and support the high purity of these samples. The position of the hydroxyl stretching band at 3631 cm^{-1} is typical for Al-rich dioctahedralaluminosilicates (Na-clay). Well resolved OH bending bands near 913 cm^{-1} (AlAlOH) and 848 cm^{-1} (AlMgOH) reflect

that the octahedral Al is partially substituted with Mg. The band at 1039 cm^{-1} is due to Si–O stretching vibrations and the bands at 523 cm^{-1} and 467 cm^{-1} are assigned to Si–O–Al and Si–O–Si bending vibrations, respectively. The absorption near 623 cm^{-1} present only in the spectra of Al-rich montmorillonites, can be ascribed either to vibrations of hydroxyl groups perpendicular to the plane of aluminosilicatelayers, or to an Al–O–R (R=Mg, Al) vibration of octahedral atoms. Clearly, the features at ~3400 cm^{-1}may be assigned to OH stretching vibrations of adsorbed water, which, in small amounts, remained in the sample even after drying at 140°C.

The FTIR spectrum of the Fe-clay shows a broad OH stretching band at 3573 cm^{-1}, which reflects the high content of octahedral Fe in the sample. This is further supported by the observation of OH-bending vibrations in the 950-800 cm^{-1} spectral region, at 874 and 820 cm^{-1}, due to AlFeOH and FeFeOH groups, respectively. An intensive Si–O stretching band is observed at 1028 cm^{-1}. In addition, three absorption bands were observed in the Si–O bending region: Si–O–Fe at 496 and 427 cm^{-1}, and Si–O–Si at 454 cm^{-1}. The feature near 687 cm^{-1} is attributed to Fe–O out-of-plane vibrations.

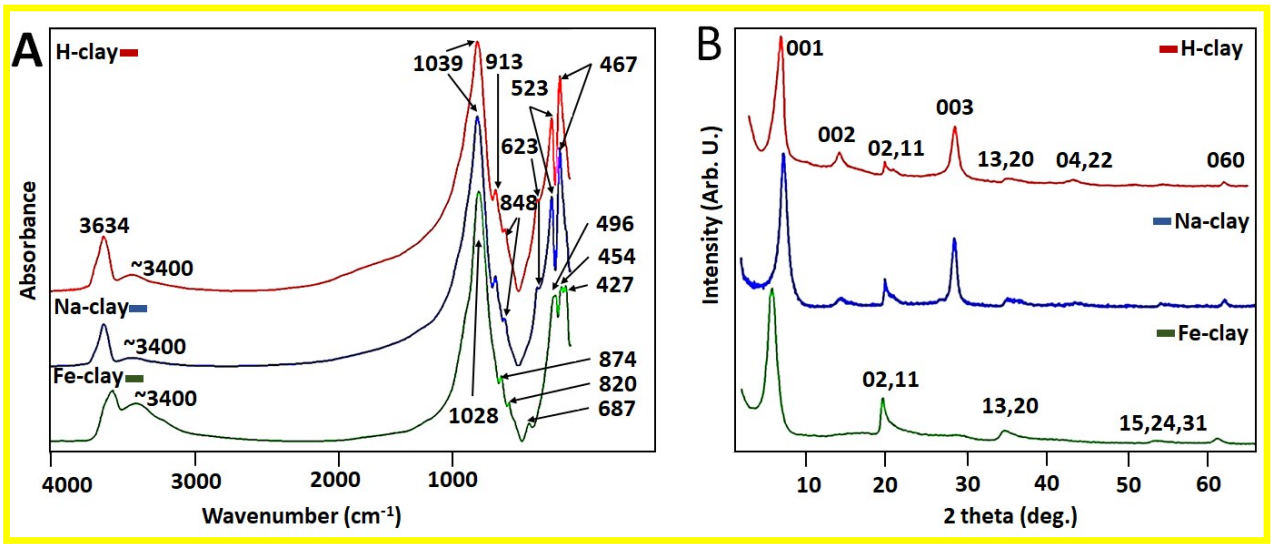

FigureS1: FTIR spectrum (panel A) and powder X-ray diffractogram (panel B) of the clays used in this study

The XRD patterns, shown in Figure S1, Panel B, did not show the presence of any crystalline trace impurities and were in accordance with the observations inferred from IR-spectroscopy. The untreated Na–clay sample exhibited a well-defined and very intense 001 peak, two higher-order reflections (003 and 004) and four non-basal *hk* diffractions (02*l*, 13*l*, 04*l*, 060).

The diffraction patterns of clays show strong basal 001 reflection at 1.51 nm (Fe-clay), 1.22 nm (Na–clay) and 1.27 nm (H–clay), which reflect the nature of interlayer cations. The non-basal reflections (*hk* bands) take the form of broad and diffuse maxima, which are typically asymmetrical towards the higher angles, arising from the randomness of the layer stacking in the *xy* plane. The non-basal reflections are invariant, regardless of the water content or the extent of intercalation between the clay layers.

SII. Thermolysis

Samples were heated to 160 °C for 24 hours, under reflux condenser cooled by water (FigureS2). After thermolysis the samples were macerated by methanol for 2 hours and then evaporated by vacuum and slight air flow at a pressure of 1 atm. The apparatus used for evaporation was connected to a dry ice trap in order to trap formamide vapours.

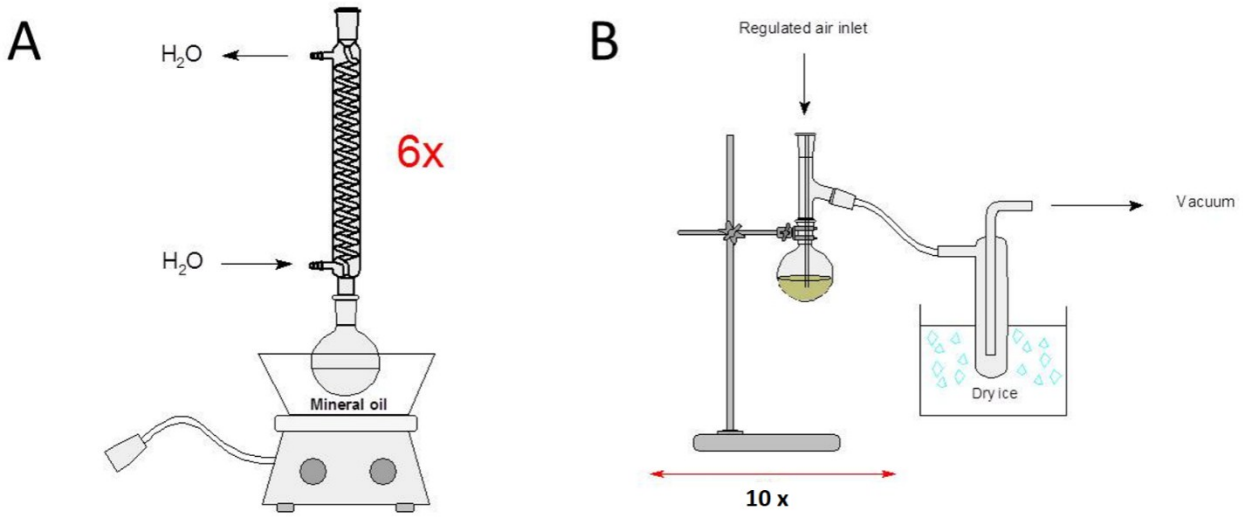

FigureS2: Experimental setup used for thermolysis (panel A) and for evaporation of formamide under low pressure and stream of air (panel B)

SIII. Methods used for product analysis

Solid residues of the samples dried under vacuum were analyzed with **GC-MS** (**Gas Chromatography combined with Mass Spectrometry) technique**. The measurements were performed using a Trace 1300 GC chromatograph coupled with an MS 1100 (Thermo Scientific, USA) ion trap mass spectrometer. A nonpolar TraceGOLD TG-5MS capillary column (Thermo Scientific, USA; 95 % (wt/wt) dimethylpolysiloxane and 5 % (wt/wt) fenylmethylpolysiloxane) was used for the chromatographic separation.

Evaporates were derivatized by a mixture of pyridine (99.9 %, Sigma Aldrich, CAS 110-86-1) and MTBSTFA (99 %, Sigma Aldrich, CAS 77377−52−7) at a ratio of 3:1, for 2 hours at 110 °C, in 1,5 mL glass vials. The derivatization enabled formation of volatile trimethylsilyl-(TMS) derivatives, measurable via GC-MS methods. Separation and detection of nucleobases, glycine and urea TMS derivatives were carried out under the same conditions. Samples of 1 μL were injected manually at split flow 100 mL/min and split rate 100 into an injector homogeneously heated at 250 °C. Helium of 99,996% purity was used as carrier gas at a flow rate of 1 mL/min. The samples were analysed using a column temperature range of 180 to 280 °C, with the initial and final temperature held for 2 min, the heating rate was set to 10 °C min^{-1}. The conditions of mass spectra measurements were as follows: transfer line temperature was 250°C, ion source temperature was 200°C and EI ionization at 70 eV was used.

The assignment of analytes and their concentrations were performed by comparing retention times, MS fragmentation patterns and band intensities for specific m/z ratio to those obtained using commercial standards: uracil (99%, Sigma Aldrich, CAS 66-22-8), thymine (99%, Sigma Aldrich, CAS 50-89-5), cytosine (99%, Sigma Aldrich, CAS 71-30-7), adenine (99%, Sigma Aldrich, CAS 73-24-5), guanine (98%, Sigma Aldrich, CAS 73-40-5), urea (BioReagent, for molecular biology, Sigma Aldrich, CAS 57-13-6), glycine (Sigma Aldrich, CAS 56-40-6) and guanidine hydrochloride (98%, Sigma Aldrich, CAS 50-01-1). External standard quantitation was performed.

Gas phase reaction products were examined with **Fourier Transform High Resolution Spectroscopy** using a Bruker IFS 125 HR spectrometer (see FigureS3) equipped with a KBr

beamsplitter and nitrogen cooled LN-MCT (Hg-Cd-Te) detector. The MCT and InSb detectors covered the spectral range of 680-4000 cm^{-1}. We worked with a spectral resolution of 0.02 cm^{-1} and the number of single scans was set to 300. For the quantification, calibration standards have been used as follows: HCN (Messer Technogas, 186 ppm/He), CO (Linde Gas, 5.3), CO_2 (Linde Gas, 5.3) and NH_3(Linde Gas, 3.8). Sample of formamide was heated in presence of catalysts in a furnace equipped with Kanthal wire in a quartz tube up to temperature of 160 ^oC in vacuum. After 60 minutes, the gas phase was transferred to a multipass White cell with optical path of 30 m and inspected by FTIR.

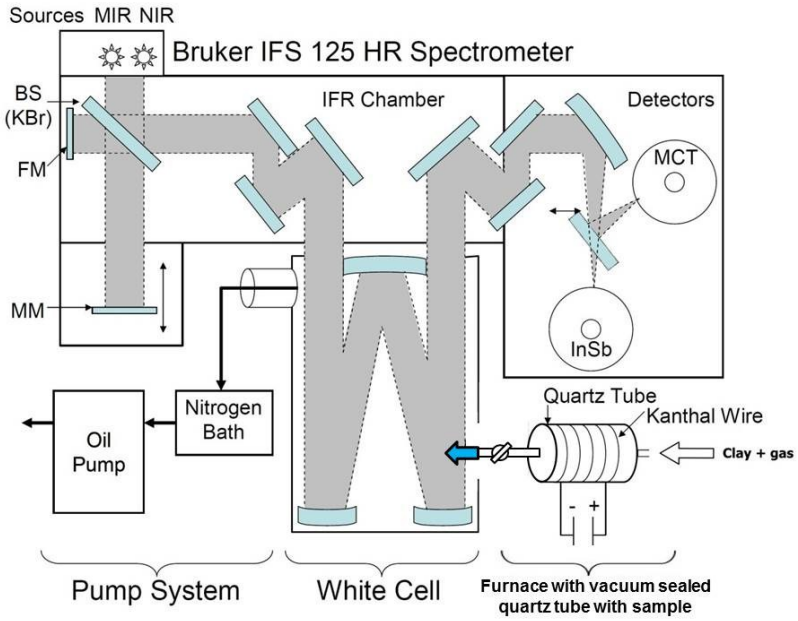

FigureS3: Scheme of the set up used for the inspection of gas phase formed in the formamide thermal decomposition experiment. BS: beamsplitter, IFR: interferometer, MM: mobile mirror, FM: fixed mirror.

Capillary electrophoretic analyses were performed by CE 7100 (Agilent technologies, Waldbronn, Germany) with UV absorbance detection at 254 nm. Fused silica capillary with internal diameter of 75 μm and with the total length of 64.5 cm was used. Hydrodynamic injection of 40 mbar for 5s and 15 kV separation voltage was applied. 40 mM sodium borate buffer pH 9.8 containing 60 mM SDS was used as a separation electrolyte (BGE). After each analysis, the capillary was flushed (120s) by BGE.The assignment of analytes was performed using commercial standards: uracil (99%, Sigma Aldrich, CAS 66-22-8), thymine (99%, Sigma

Aldrich, CAS 50-89-5), cytosine (99%, Sigma Aldrich, CAS 71-30-7), adenine (99%, Sigma Aldrich, CAS 73-24-5), guanine (98%, Sigma Aldrich, CAS 73-40-5), urea (BioReagent, for molecular biology, Sigma Aldrich, CAS 57-13-6), glycine (Sigma Aldrich, CAS 56-40-6) and guanidine hydrochloride (98%, Sigma Aldrich, CAS 50-01-1).

SIV. GC-MS Detection of nucleobases and other prebiotic substances

We provide a series of 20 comparative chromatograms and corresponding mass spectra for the Sample no. 2, Fe-Clay and standards. In the similar manner, all the 100 records for each sample have been compared with 10 standards of adenine, guanine, cytosine, thymine, uracil, purine, hypoxanthine, guanidine, urea and glycine. 91 detections have been successful. For Samples 6, 7, 9 and 10, several products have not been discovered at the typical detection threshold of 10^{-2}ppmV.

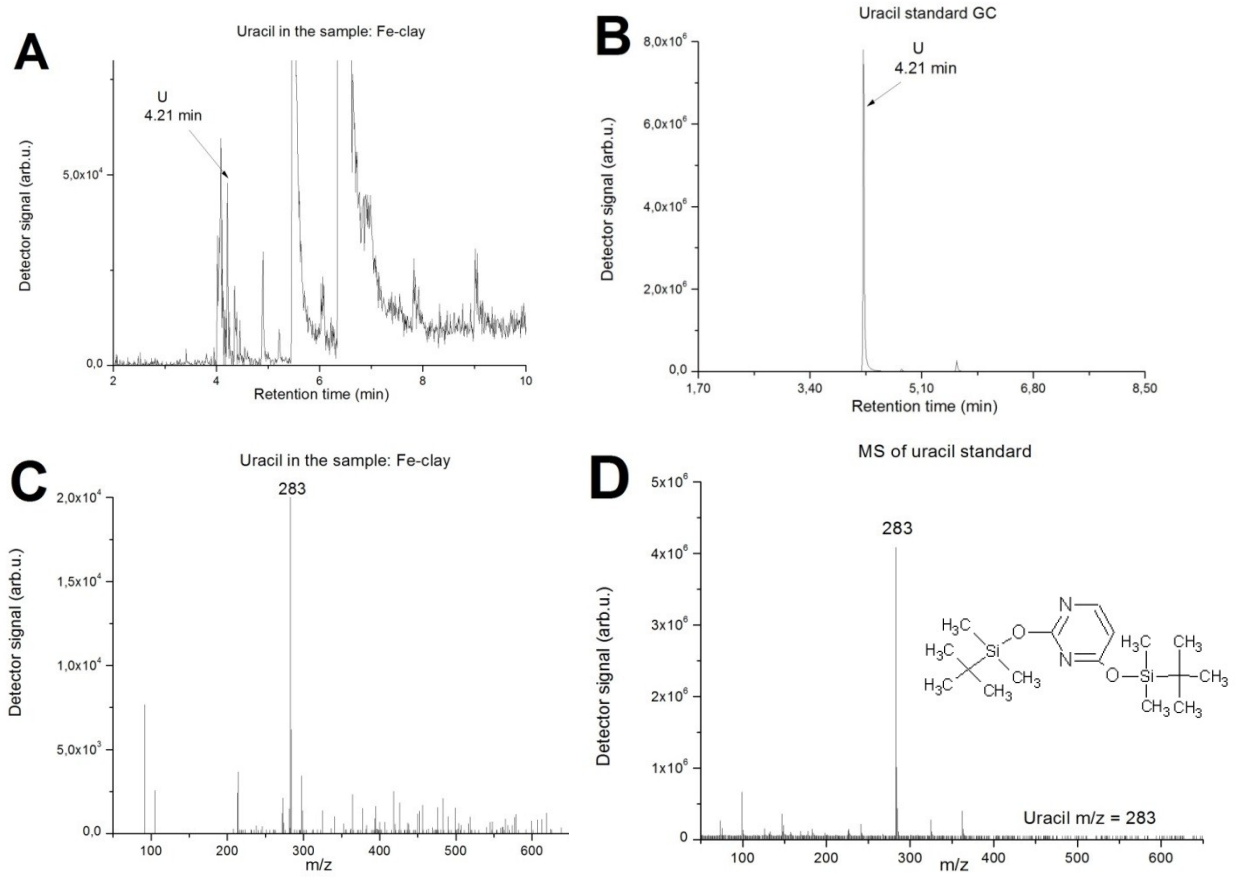

Figure S4. Uracil detected in the sample from thermolysis of formamide in presence of Fe-clay (experiment no. 2 in Table 1, main text). Panel A depicts chromatogram with assignment of corresponding peak of uracil. Panel B depicts chromatogram with assignment of corresponding peak of uracil for standard. Panel C shows mass spectrum of uracil with retention time t = 4.21 min. and typical peak at m/z = 283, and panel D shows the mass spectrum of the derivatized standard.

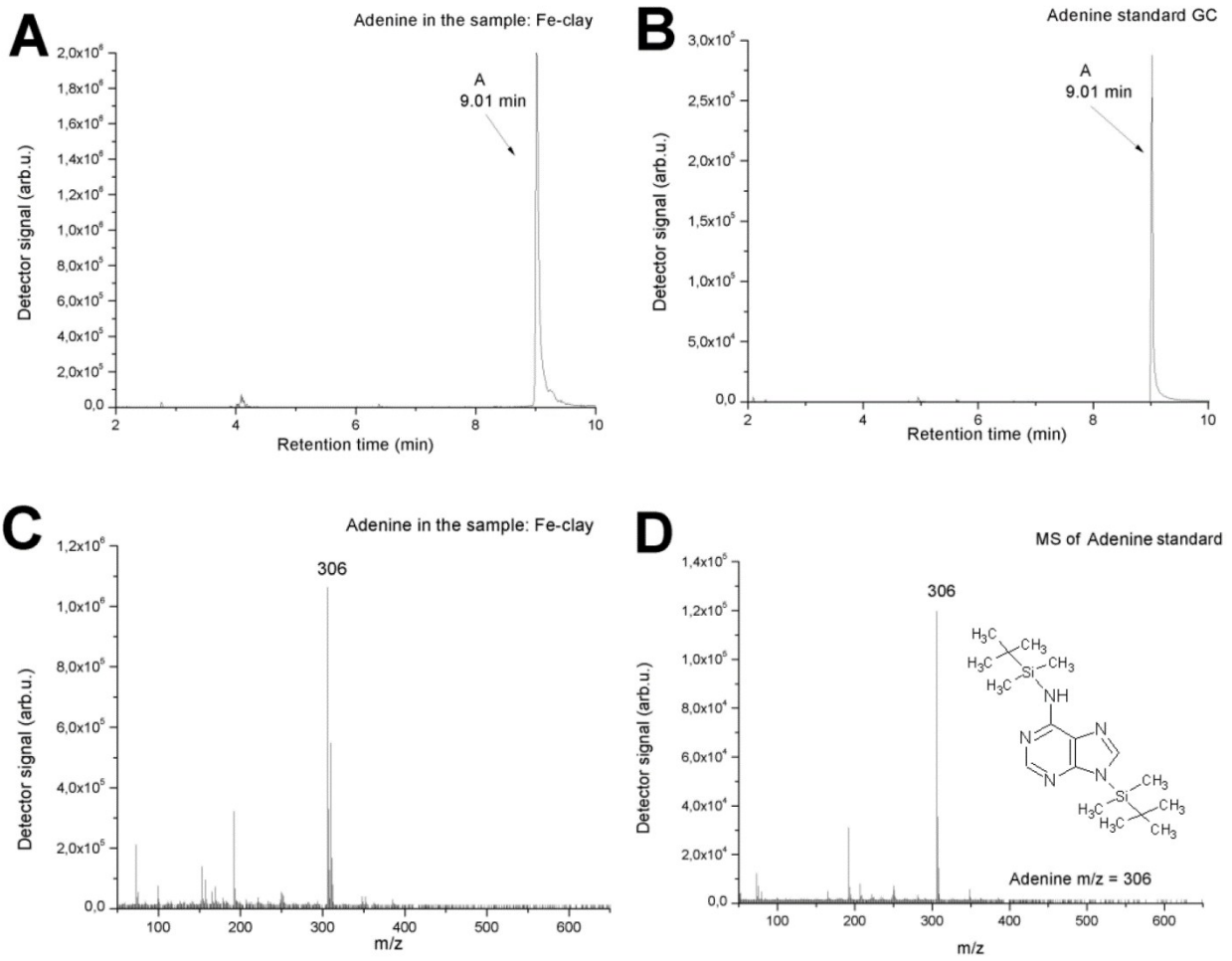

Figure S5. Adenine detected in the sample from thermolysis of formamide in presence of Fe-clay (experiment no. 2 in Table 1, main text). Panel A depicts chromatogram with assignment of corresponding peak of adenine. Panel B depicts chromatogram with assignment of corresponding peak of adenine for standard. Panel C shows mass spectrum of adenine with retention time t = 9.01 min. and typical peak at m/z = 306,and panel D shows the mass spectrum of the derivatized standard.

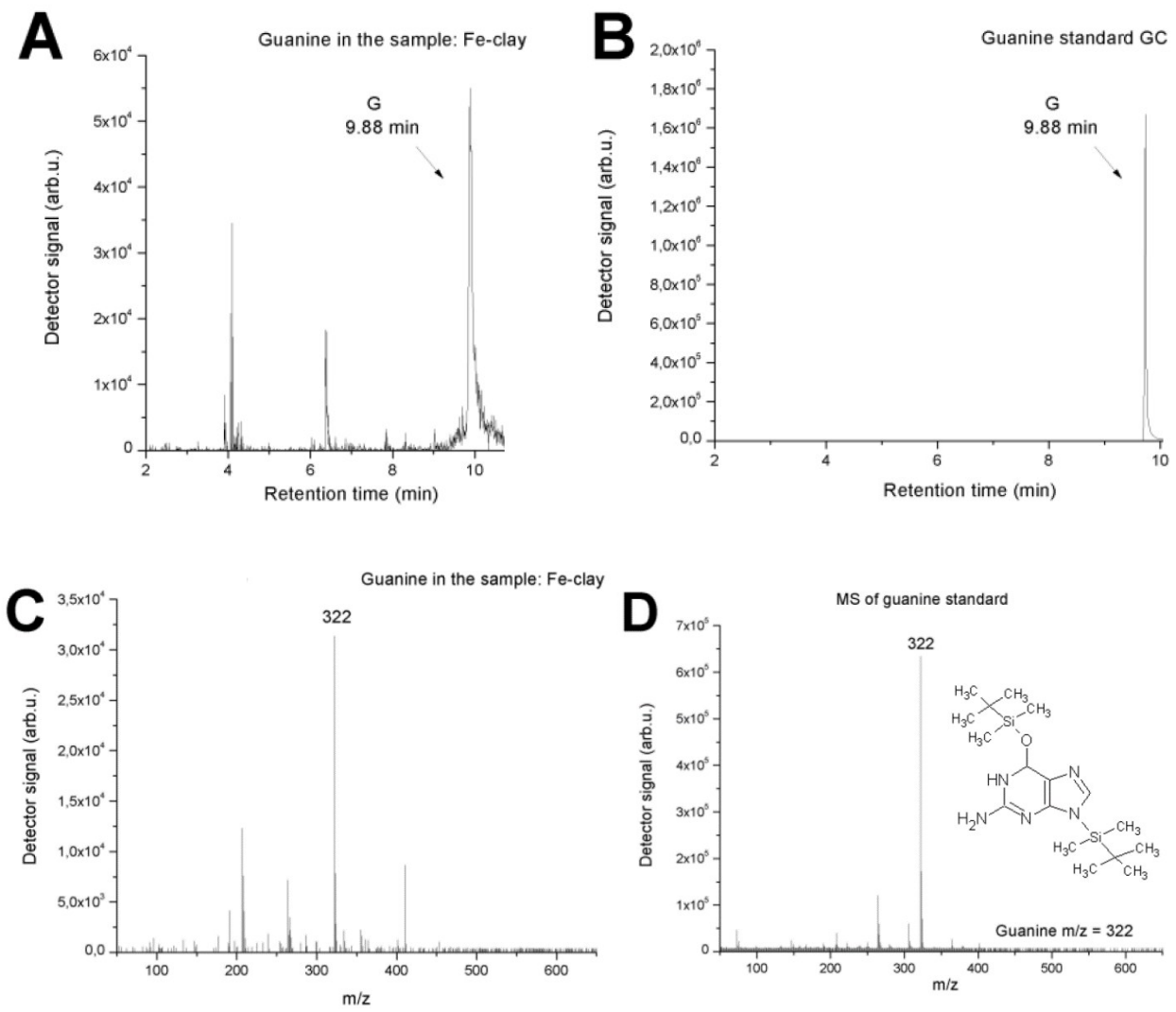

Figure S6. Guanine detected in the sample from thermolysis of formamide in presence of Fe-clay (experiment no. 2 in Table 1, main text). Panel A depicts chromatogram with assignment of corresponding peak of guanine. Panel B depicts chromatogram with assignment of corresponding peak of guanine for standard. Panel C shows mass spectrum of guanine with retention time t = 9.88 min. and typical peak at m/z = 322, and panel D shows the mass spectrum of the derivatized standard.

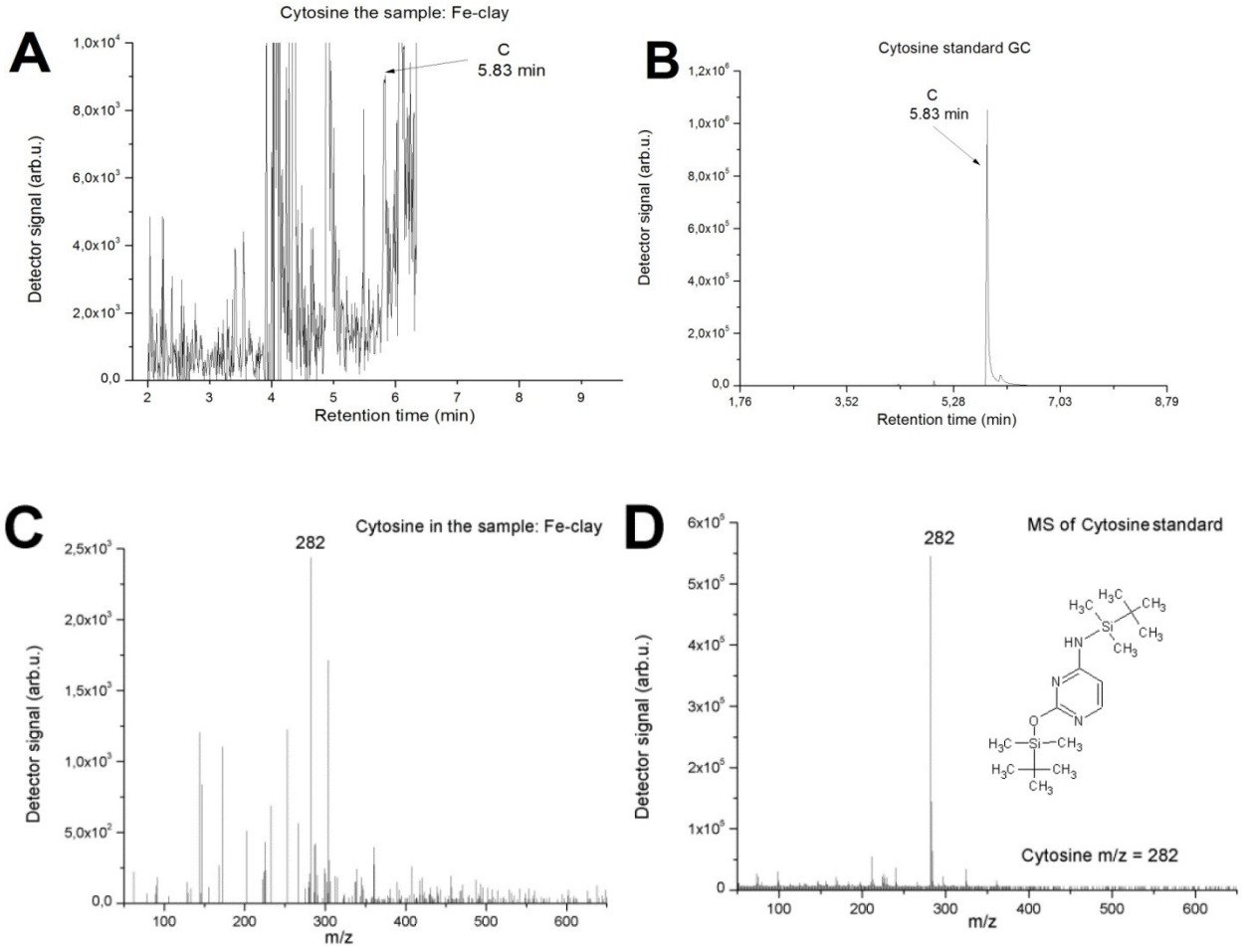

Figure S7. Cytosine detected in the sample from thermolysis of formamide in presence of Fe-clay (experiment no. 2 in Table 1, main text). Panel A depicts chromatogram with assignment of corresponding peak of cytosine. Panel B depicts chromatogram with assignment of corresponding peak of cytosine for standard. Panel C shows mass spectrum of cytosine with retention time t = 5.83 min. and typical peak at m/z = 282. Panel D shows the mass spectrum of the derivatized standard.

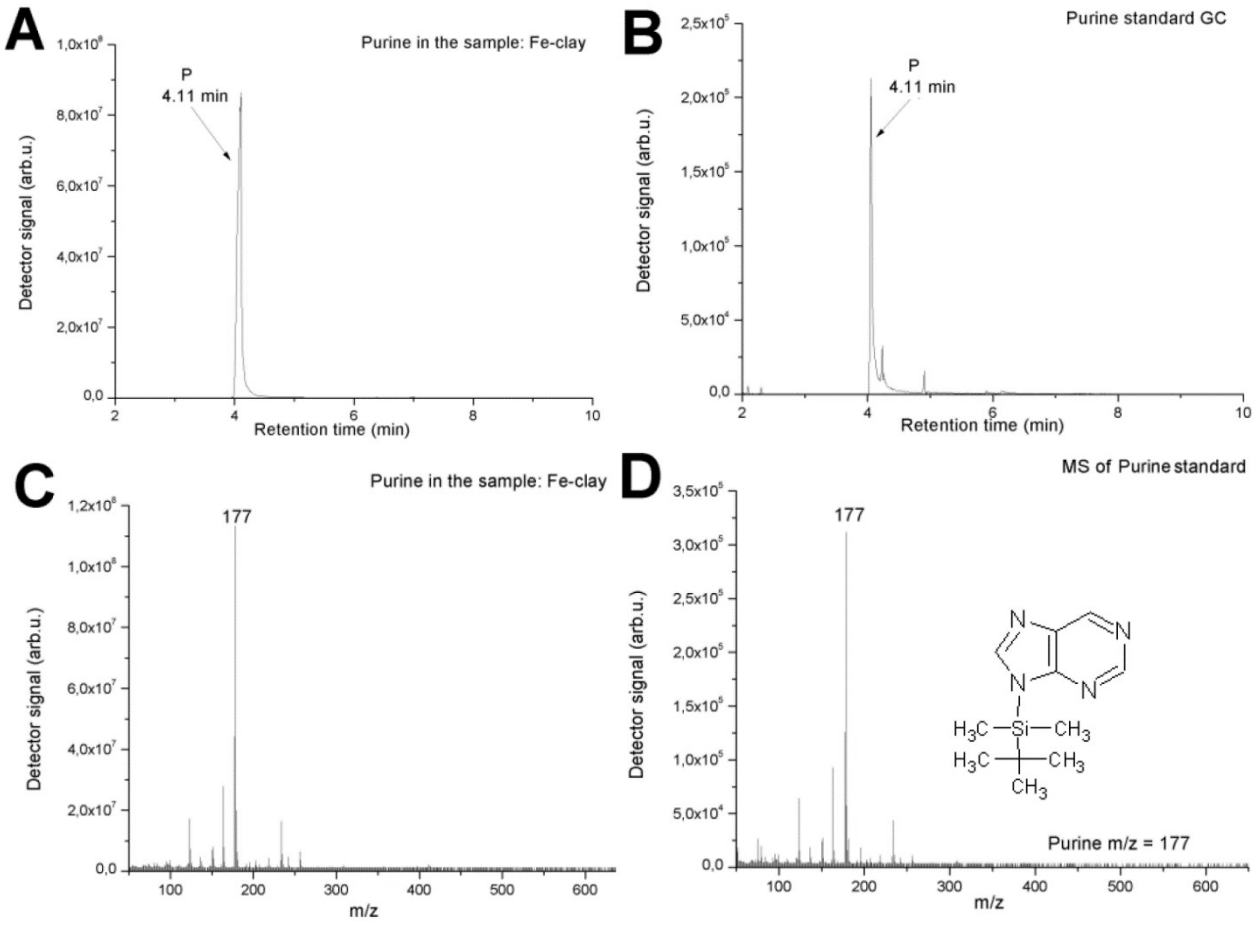

Figure S8. Purine detected in the sample from thermolysis of formamide in presence of Fe-clay (experiment no. 2 in Table 1, main text). Panel A depicts chromatogram with assignment of corresponding peak of purine. Panel B depicts chromatogram with assignment of corresponding peak of purine for standard. Panel C shows mass spectrum of purine with retention time t = 4.11 min. and typical peak at m/z = 177. Panel D shows the mass spectrum of the derivatized standard.

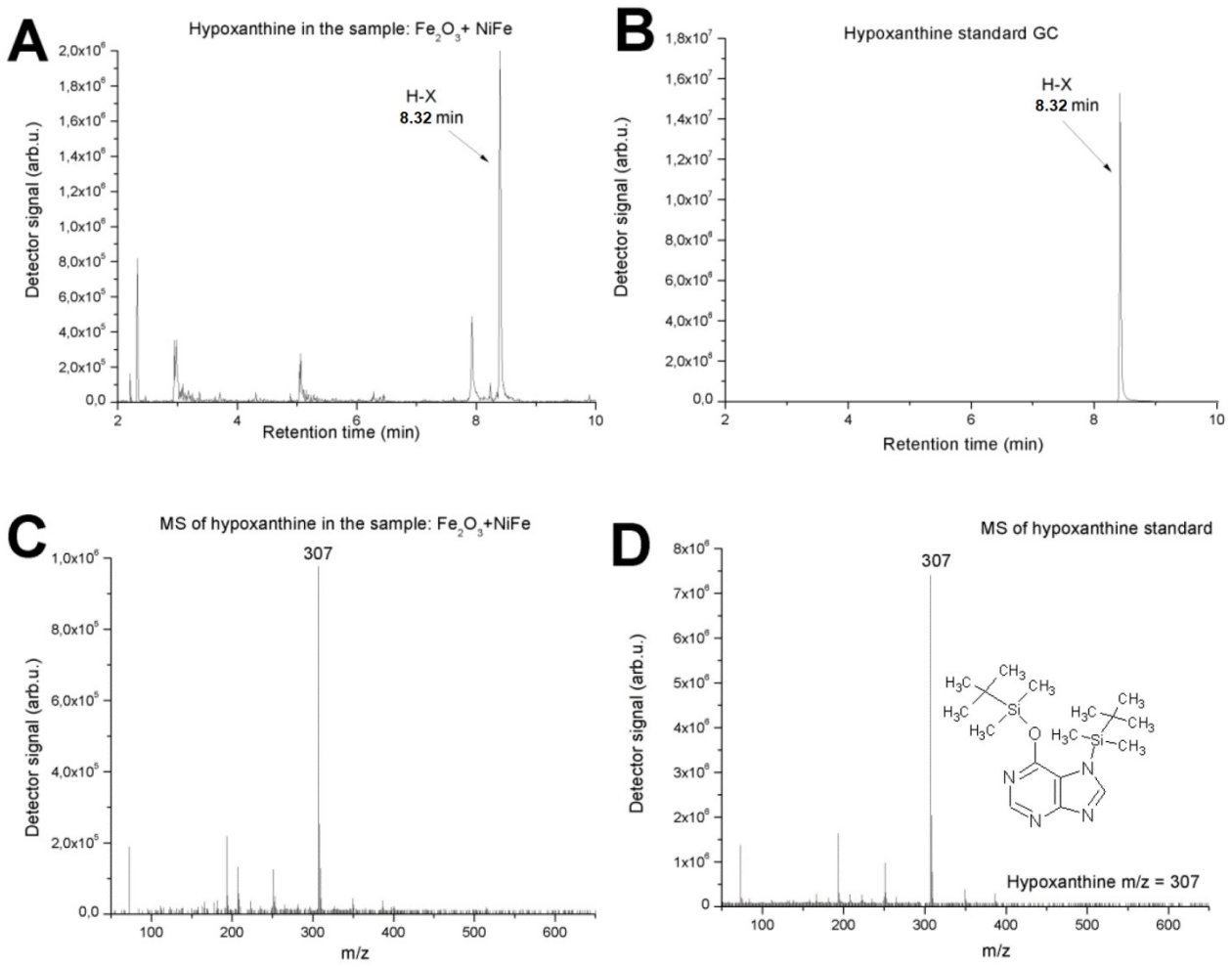

Figure S9. Hypoxanthine detected in the sample from thermolysis of formamide in the presence of Fe-clay (experiment no. 2 in Table 1, main text). Panel A depicts chromatogram with assignment of corresponding peak of hypoxanthine. Panel B depicts chromatogram with assignment of corresponding peak of hypoxanthine for standard. Panel C shows mass spectrum of hypoxanthine with retention time t = 8.32 min. and typical peak at m/z = 307. Panel D shows the mass spectrum of the derivatized standard.

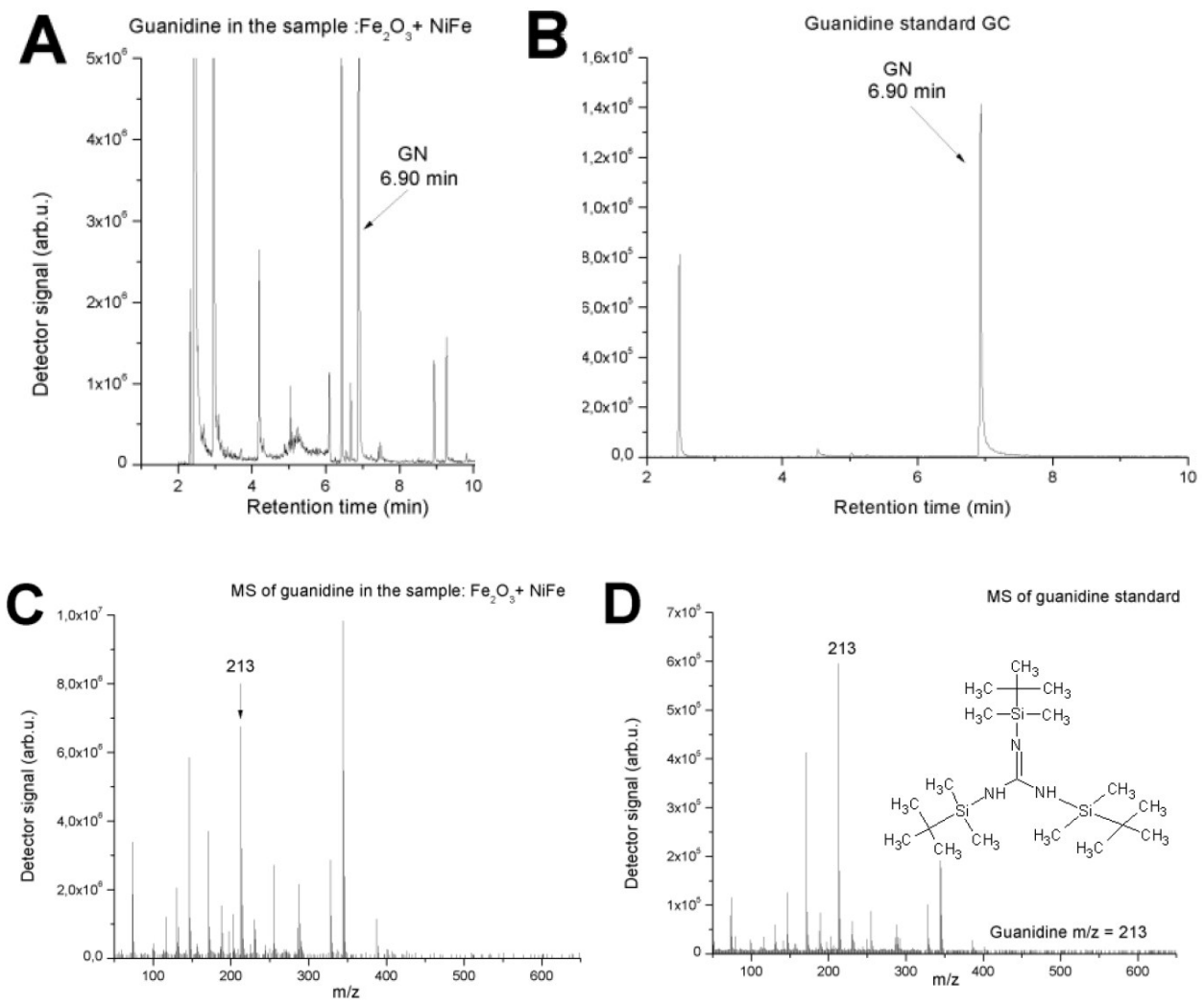

Figure S10. Guanidine detected in the sample from thermolysis of formamide in the presence of Fe_2O_3 mixed with NiFe meteorite (experiment no. 2 in Table 1, main text). Panel A depicts chromatogram with assignment of corresponding peak of guanidine. Panel B depicts chromatogram with assignment of corresponding peak of guanidine for standard. Panel C shows mass spectrum of guanidine with retention time t = 6.90 min. and typical peak at m/z = 213, and panel D shows the mass spectrum of the derivatized standard.

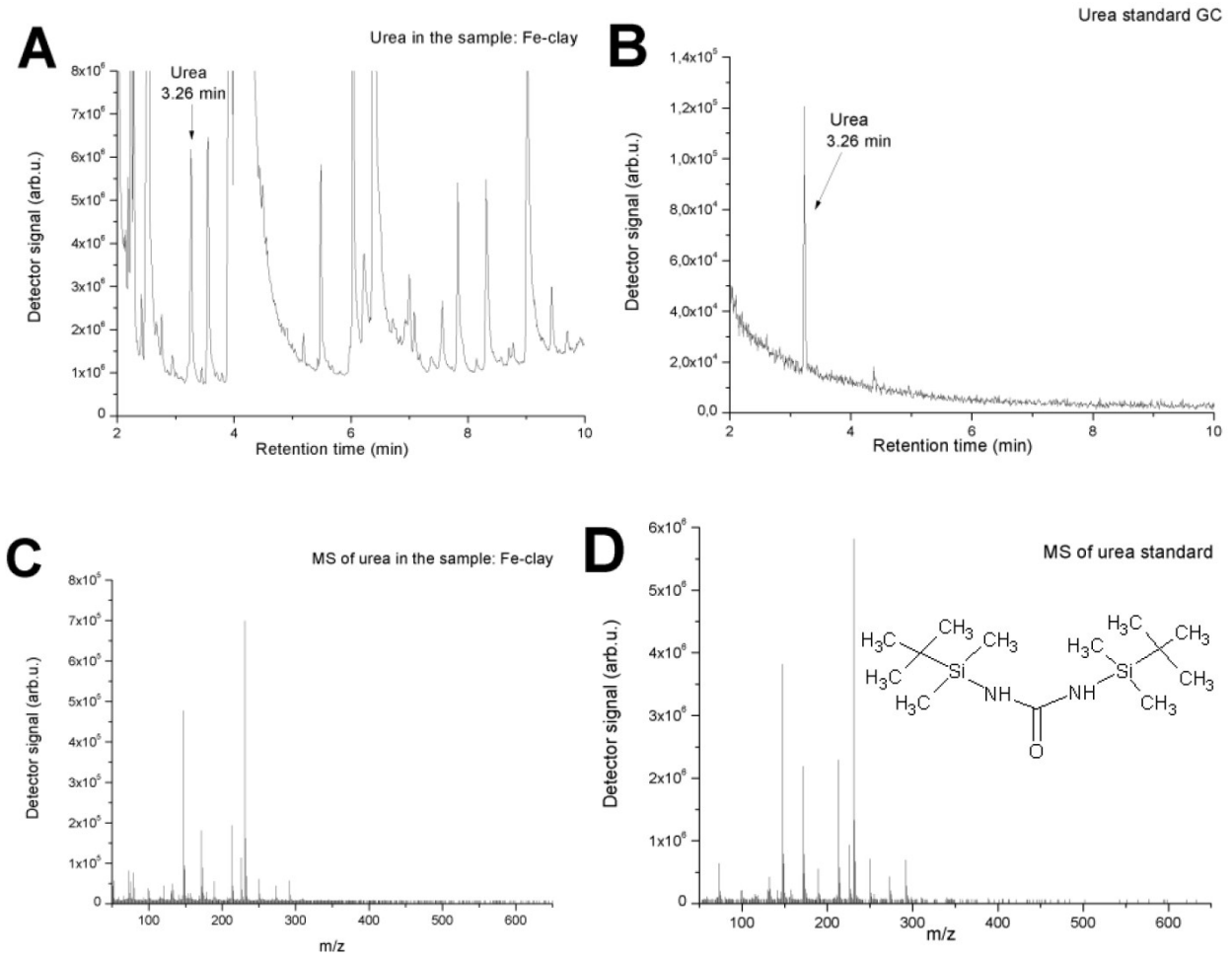

Figure S11. Urea detected in the sample from thermolysis of formamide in presence of Fe_2O_3 mixed with NiFe meteorite (experiment no. 2 in Table 1, main text). Panel A depicts chromatogram with assignment of corresponding peak of urea. Panel B depicts chromatogram with assignment of corresponding peak of urea for standard. Panel C shows mass spectrum of urea with retention time t = 3.26 min. and peak at m/z = 231, and panel D shows the mass spectrum of the derivatized standard.

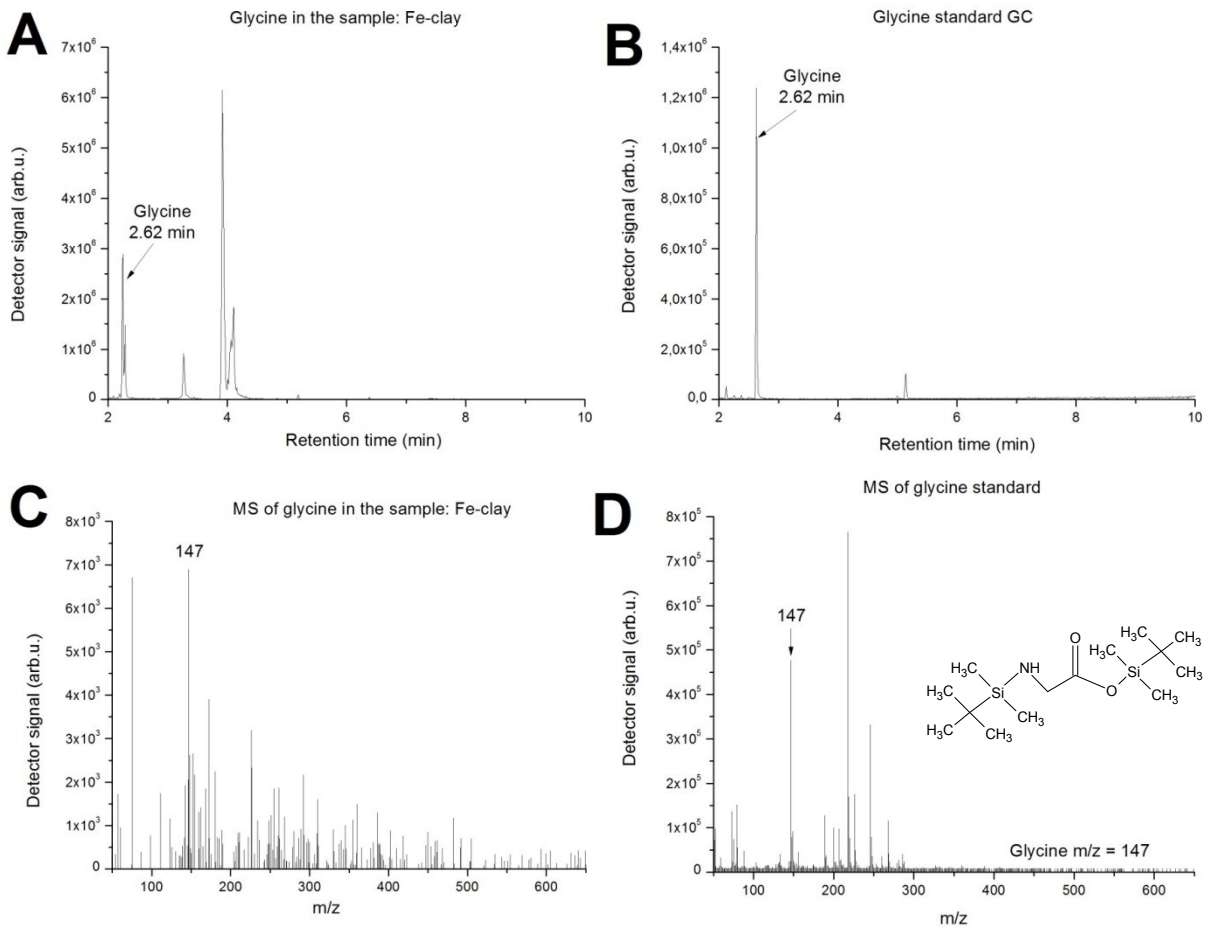

Figure S12. Glycine detected in the sample from thermolysis of formamide in the presence of Fe_2O_3 mixed with NiFe meteorite (experiment no. 2 in Table 1, main text). Panel A depicts chromatogram with assignment of corresponding peak of glycine. Panel B depicts chromatogram with assignment of corresponding peak of glycine for standard. Panel C shows mass spectrum of glycine with retention time t = 2.62 min. and typical peak at m/z = 147, and panel D shows the mass spectrum of the derivatized standard.

SV. Contamination

Regarding the possible contamination, we have performed a comparative analysis of blanks. The blanks are compared with a chromatogram of Sample 2 (formamide and Fe-clay). We have conducted reference experiment without heating with Fe-clay used as a catalyst (Panel B, chromatogram a), and we have not detected any one nucleobase. We have also tested nucleobases in water after washing of the vessel touched with finger without gloves (Panel B, chromatogram b) and water washed from montmorillonite catalyst (Panel B, chromatogram c). We obtained negative results. We show 3 blank chromatograms.

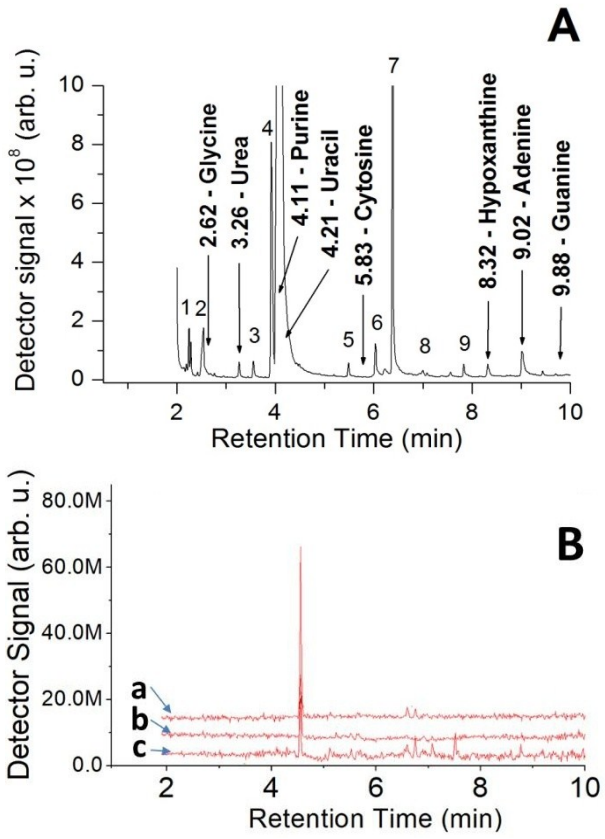

Figure S13. Chromatogram of formamide heated in presence of Fe-clay (panel A) and the blank measurements (panel B), detection was made after derivatization. For details, see the text above.

Further, let us not that the ppm amounts of nucleobases found in our samples imply ng.µl^{-1} concentrations of nucleic acids. Such concentrations are usually observed during standard plasmid DNA extraction and purification from *E. coli*. It is very difficult to imagine that such a high concentration normally achievable only after a specially designed purification process would be a result of a simple contamination of the studied samples.